LETTERS
PUBLISHED ONLINE: 9 AUGUST 2009 | DOI: 10.1038/NMAT2508
nature materials

Surface-induced crystallization in supercooled tetrahedral liquids

Tianshu Li[1]*, Davide Donadio[1], Luca M. Ghiringhelli[2] and Giulia Galli[1]

Surfaces have long been known to have an intricate role in solid–liquid phase transformations. Whereas melting is often observed to originate at surfaces, freezing usually starts in the bulk, and only a few systems have been reported to exhibit signatures of surface-induced crystallization[1]. These include assembly of chain-like molecules[2], some liquid metals and alloys[3–5] and silicate glasses[6,7]. Here, we report direct computational evidence of surface-induced nucleation in supercooled liquid silicon and germanium, and we illustrate the crucial role of free surfaces in the freezing process of tetrahedral liquids exhibiting a negative slope of their melting lines ($dT/dP|_{coexist} < 0$). Our molecular dynamics simulations show that the presence of free surfaces may enhance the nucleation rates by several orders of magnitude with respect to those found in the bulk. Our findings provide insight, at the atomistic level, into the nucleation mechanism of widely used semiconductors, and support the hypothesis of surface-induced crystallization in other tetrahedrally coordinated systems, in particular water in the atmosphere.

Melting and freezing are very common and widely studied phenomena, yet fundamental questions such as the role of surfaces during crystallization and, in particular the underlying microscopic mechanism are not well understood. Nucleation processes have an important role in a variety of scientific disciplines, such as atmospheric physics[8–10], metallurgy[4] and nanoscience[11]. However, technical difficulties in designing experiments to capture nucleation events have so far prevented an accurate characterization of freezing processes, and direct simulations of nucleation require very challenging computer experiments[12–14].

Simple thermodynamic arguments suggest that complete surface freezing is unlikely to occur in common elemental substances[15], and incomplete surface crystallization may be favoured only when a crystalline surface can be partially wet by its own melt[8,16]. However, surface-induced crystallization has been observed in some liquid metals and metallic alloys[3–5]. Its occurrence has been mainly attributed to surface layering effects[17], although recent studies suggest that impurity nucleation centres may be responsible for triggering crystallization at surfaces of liquid metallic alloys[18]. Heterogeneous nucleation and elastic strain effects have been studied in depth in the case of glass-forming materials such as silicate glasses[6,7]. In colloidal systems and liquid crystals, freezing at surfaces has also been observed, and rationalized in terms of highly anisotropic interactions between molecular chains[2].

Here, we report about surface-induced crystallization in elemental, supercooled tetrahedral liquids, and we propose a mechanism for nucleation related to density changes on melting. We combined the recently developed forward flux sampling (FFS) method[19,20] with molecular dynamics simulations[21] and computed nucleation rates of diamond silicon and germanium in the supercooled liquid states, at temperatures up to 95% of the melting point. Our results provide insight not only into nucleation processes of widely used semiconductors, but also of other tetrahedrally coordinated systems, such as water.

We carried out our simulations using Tersoff[22] and Stillinger–Weber[23] potentials at temperatures up to 95% of the melting temperature T_m for Si and Ge in both bulk and slab (with two free surfaces) configurations. The rate for growing a solid cluster containing λ atoms out of the liquid can be expressed by the product of a flux rate $\dot{\Phi}_{\lambda_0}$ for the formation of smaller clusters with λ_0 ($\lambda_0 < \lambda$) atoms, and the probability $P(\lambda|\lambda_0)$ for these clusters to eventually grow to size λ. Within the FFS scheme, one can compute these two terms separately, and $P(\lambda|\lambda_0)$ is obtained by sampling a number of interfaces between the initial and final states in the space of the order parameter. In our case, it is natural to choose this parameter as the number of atoms λ contained in the largest crystalline cluster[24]. The flux rate $\dot{\Phi}_{\lambda_0}$ is computed by conducting standard molecular dynamics simulations to capture trajectories leading to the formation of small clusters. During this step, we find that inclusion of free surfaces does not significantly change the flux rates, at all temperatures. Therefore, the influence of free surfaces on nucleation rates is expected to be sufficiently well represented by the variation of the growth probability $P(\lambda|\lambda_0)$. After computing the flux rate, the entire growth process is decomposed into a series of consecutive sub-events representing the crossing of adjacent interfaces. The total growth probability $P(\lambda|\lambda_0)$ is computed by multiplying the individual crossing probabilities $P(\lambda_i|\lambda_{i-1})$ that are accessible to direct molecular dynamics simulations.

The calculated transition probability $P(\lambda_i|\lambda_{i-1})$ as a function of the cluster size λ is shown in Fig. 1a for both bulk systems and slabs, at several temperatures. Initially, $P(\lambda|\lambda_0)$ sharply decreases as small clusters grow, and then it tends to saturate, indicating the formation of a critical nucleus. Consistent with classical nucleation theory, the calculated nucleation rates show a strong dependence on T: increasing T from 0.79 T_m to 0.86 T_m yields a decrease in the rate by over 16 orders of magnitude. In particular, the computed nucleation rate $4.77 \pm 3.26 \times 10^{11}$ m^{-3} s^{-1} at 0.86 T_m agrees well with the experimental measurement 2.0×10^{10} m^{-3} s^{-1} at $14 \pm 1\%$ supercooling[25].

The most striking result of this calculation is that it demonstrates a clear transition in preferential nucleation from the bulk to the slab, as T increases. This finding is illustrated in Fig. 1b, which shows the ratio of the growth probability between the liquid slab and bulk, P_{slab}/P_{bulk}, as a function of λ. At 0.79 T_m, this ratio decreases rapidly, as the small clusters grow, and it stabilizes around 10^{-2}, for $\lambda > 100$. This indicates that nucleation from the liquid slab is unfavourable as compared with that from the bulk. When T is increased to 0.86 T_m, P_{slab}/P_{bulk} is around unity, suggesting that in the slab and the bulk one achieves virtually identical nucleation rates. As the temperature

[1]Department of Chemistry, University of California, Davis, California 95616, USA, [2]Fritz Haber Institute of the Max Planck Society, Theory Department, Faradayweg 4-6, D14195 Berlin-Dahlem, Germany. *e-mail: tsli@ucdavis.edu.

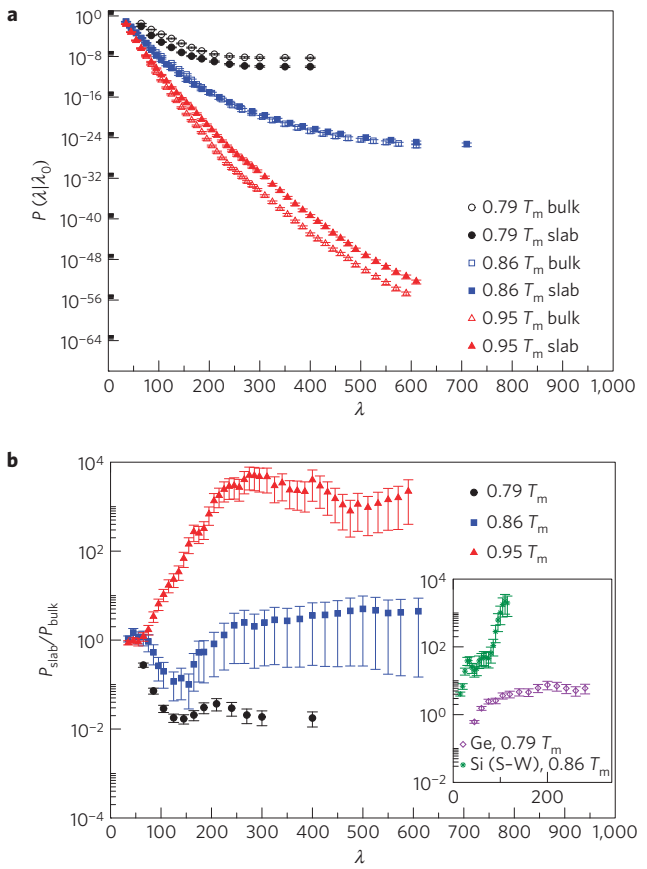

Figure 1 | Computed nucleation rates in liquid Si and Ge. a, Calculated growth probability $P(\lambda|\lambda_0)$ as a function of the cluster size in both bulk liquid Si and liquid slab using the Tersoff potential at different temperatures. λ_0 is 40 for 0.79 T_m, and 25 for 0.85 T_m and 0.95 T_m. The total simulation time for each curve is about 1 μs. Using the definition of the critical nucleus as the one that has a committor probability of 0.5 (ref. 12), that is, 50% probability of dissolving completely, the critical sizes at 0.79 T_m and 0.86 T_m are determined to be 300 ± 30 atoms and 600 ± 50, respectively. **b**, Calculated ratio of the growth probability between the liquid slab and the bulk liquid, P_{slab}/P_{bulk}, as a function of the cluster size. The inset shows the same ratios for Tersoff Ge (ref. 22) at 0.79 T_m and Stillinger–Weber[23] Si at 0.86 T_m. The error bars are computed on the basis of the binomial distribution of k_i, the number of successful trial runs at λ_i (ref. 20).

is further increased up to 0.95 T_m, the liquid slab yields a nucleation rate over a thousand times higher than that in the bulk liquid.

This noticeable increase in nucleation rates is then naturally attributed to the presence of the free surface in the slab. To show that this is indeed the case, we explore the microscopic details of growing Si clusters, particularly their distributions in the direction z normal to the free surface. Figure 2 shows such distributions at different stages of the cluster formation. Initially, the small solid Si clusters are distributed nearly evenly along the z axis (Fig. 2a), which is in accord with the computed flux rates $\dot{\Phi}_{\lambda_0}$ being of comparable magnitude in the bulk and in the slab. As solid clusters grow, we observe a clear tendency for those with the highest growth probability to be located close to the free surface. Such a tendency is confirmed by fewer clusters being present in the middle of the slab, as λ increases. Finally all clusters exclusively reside about 1 nm away from the immediate interface between the liquid and the vacuum (Fig. 2c).

The enhancement of nucleation rates found here cannot be rationalized using models proposed in the literature. First, the nucleation mechanism observed here is homogeneous, as no heterogeneous nucleation[6,18] centres such as foreign particles are present in our simulations. Second, we do not find any signature of surface layering as in the case, for example, of liquid metallic alloys[17]: for instance, the density profiles using the Tersoff potential show a smooth variation of the liquid density near the surface. Third, the 'elastic strain' proposed[7] to influence nucleation in glass-forming systems, has no significant role in Si and Ge supercooled liquids close to their melting temperatures, as these systems cannot be modelled as viscoelastic bodies. Last, the rate enhancement found in our simulations may not be explained in terms of a balance of interface free energies for complete surface freezing[15] requiring that:

$$\gamma_{lv} - \gamma_{ls} - \gamma_{sv} > 0 \quad (1)$$

or incomplete surface freezing[8,16] requiring that:

$$\gamma_{sv} - \gamma_{lv} - \gamma_{ls} < 0 \quad (2)$$

where γ_{sv}, γ_{lv} and γ_{ls} are solid–vacuum, liquid–vacuum and liquid–solid surface tension, respectively. By using $\gamma_{lv} = 0.60 \pm 0.03\ \mathrm{J\,m^{-2}}$ computed in our simulations (see Supplementary Information for details) and the reported values for $\gamma_{sv} = 1.25\ \mathrm{J\,m^{-2}}$ (ref. 26) and $\gamma_{ls} = 0.40 \pm 0.01\ \mathrm{J\,m^{-2}}$ (ref. 27) at 0.95 T_m for Tersoff Si, one finds that neither condition (1) nor (2) is satisfied.

To understand the role of the liquid surface in crystallization events, we consider the nucleation rate

$$R = A \exp(-\Delta G^*/k_B T)$$

where A is a kinetic pre-factor proportional to the self-diffusion coefficient[28] and ΔG^* is the free energy barrier. The increase in nucleation rate can result either from an increase of the pre-factor A or a decrease of ΔG^*. If kinetic effects were to have a dominant role, the ratio of surface to bulk self-diffusion coefficients would have to increase by several orders of magnitude in going from 0.79 T_m to 0.95 T_m. In fact, at all of the temperatures considered in our work, the diffusion coefficients of Si in the slab and the bulk are of the same order of magnitude. This indicates that kinetic contributions to the rate enhancement are not significant. On the other hand, the nucleation rate is very sensitive to the change of the free energy barrier ΔG^*. The free energy change ΔG for the formation of a small crystallite is the sum of the volume contribution ΔG_v and the solid–liquid interface contribution ΔG_i:

$$\Delta G = \Delta G_v + \Delta G_i$$

We note that in the liquid slab the solid Si clusters reside in the subsurface (see Fig. 2c,d) and are thus still surrounded by a liquid-like environment; therefore, the variation of the solid–liquid interface contribution ΔG_i is expected not to be significant, compared with ΔG_v. The volume contribution ΔG_v is instead decreased, as compared with the bulk. In particular in our simulations we find that the free surface introduces a small lateral pressure ($p < 0$), in the plane parallel to the surface. The lateral pressure is directly related to the liquid–vacuum surface tension γ_{lv}, according to its mechanical definition. Therefore, a pressure-dependent term $\delta G_v(p)$ must be added to the volume free energy change ΔG_v, to account for the nucleation of a cluster containing λ atoms:

$$\delta G_v(p) = \frac{\lambda p(\rho_L - \rho_S)}{\rho_L \rho_S}$$

where ρ_L and ρ_S are the number densities of the liquid and solid, respectively. As liquid Si is denser than the solid at the melting point, that is, $\rho_L > \rho_S$, $\delta G_v(p)$ is negative. It then follows that

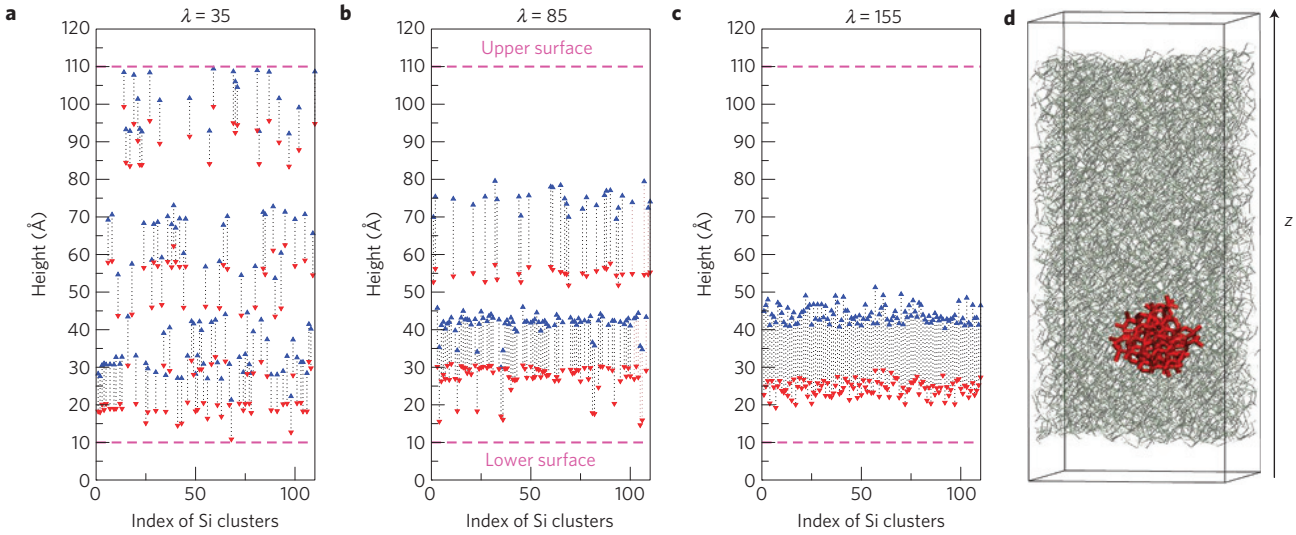

Figure 2 | Growth of Si crystallites at 0.95 T_m. a–c, Distributions of solid Si crystallites normal to the free surface in the Si liquid slab as a function of the cluster size $\lambda = 35$ (**a**), $\lambda = 85$ (**b**) and $\lambda = 155$ (**c**) at 0.95 T_m. Each vertical pair of blue (red) up (down) triangles connected by a dashed line represents the upper (lower) boundaries of a solid Si cluster. **d**, A snapshot of a solid Si cluster (red) containing 155 Si atoms (corresponding to one of the configurations in **c**) surrounded by liquid Si (grey line) in the slab with two free surfaces, normal to the z direction. The distributions show asymmetric behaviours due to both the finite sampling at each interface λ_i and the asymmetries of instantaneous fluctuations. Note that FFS identifies only the fastest trajectories leading to crystallization.

the energy barrier for nucleation is slightly lowered near a liquid surface, relative to that in the bulk where $p = 0$. A rough estimate of $\delta G_v^*(p)$ at 0.95 T_m (see the Methods section) yields an increase of nucleation rates of $10^3 \sim 10^5$, consistent with the calculated P_{slab}/P_{bulk}. In other words, in a liquid with $dT/dP|_{coexist} < 0$, the density is decreased on solidification, and thus the presence of a free surface can accommodate volume expansion more easily owing to surface tension, and nucleation in its vicinity may be preferred. To further elucidate the role of surface tension, we repeated the simulations in the bulk at 0.95 T_m, but with a small negative hydrostatic pressure applied to the cell ($p \sim -1.8$ kbar, that is, the same p corresponding to the surface tension in the slab). This is equivalent to lowering the density of the liquid, bringing it closer to that of the solid (see Fig. 3). As shown in Fig. 4, the slight decrease in liquid density in the bulk reproduces essentially the observed increase of nucleation rates in the liquid slab.

The calculated temperature-dependent density change, as obtained for the Tersoff Si, is shown in Fig. 3 for both the liquid and the solid near T_m. Note that at all T in our simulation, the liquid slab is under tension, as a result of the presence of surfaces. At 0.95 T_m, liquid Si is about 1% denser than the solid. Hence the formation of a less-dense solid Si nucleus is easier in the proximity of a surface. At 0.79 T_m, the density of supercooled liquid falls below that of the solid. In this case, nucleation at the surface involves a higher energy barrier than in the bulk, and is therefore not preferred. We also notice that the densities of diamond and liquid Si become equal at about 0.86 T_m, where our simulations show no difference in rates between surface and bulk nucleation. To further elucidate the role of density, we also conducted simulations for Ge at 0.79 T_m using the Tersoff potential, and for Si at 0.86 T_m using the Stillinger–Weber potential[23]. In both cases, the liquids are denser than the solids, with 3% and 7% density difference, for the Tersoff Ge and Stillinger–Weber Si, respectively. Calculations show (see Fig. 1b, inset) that freezing in the slab is still preferred for both systems, consistent with our analysis, and our results for Tersoff Si.

Although we found conditions under which crystallization is favoured by the presence of free surfaces, we emphasize that nucleation does not occur exactly at the surface but instead in a subsurface region that is a few atomic layers underneath. The

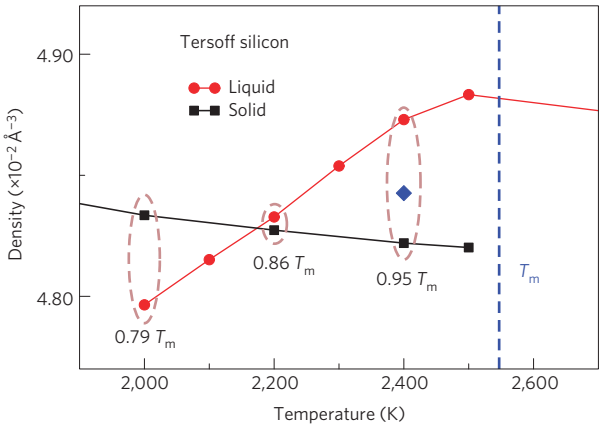

Figure 3 | Densities of liquid and diamond cubic silicon modelled by the Tersoff potential as functions of temperature near the melting point T_m. The blue diamond represents the density of liquid Si under a negative pressure $p = -1.8$ kbar at 0.95 T_m.

distribution of the lateral pressure $p_T(z)$ normal to the free surfaces (see Supplementary Information for details) shows that the cluster tends to grow in the region where the pressure field is negative, however not where the pressure field exhibits its minimum, which occurs very close to the surface. From thermodynamic arguments[16], nucleation occurs in the immediate proximity of the surface only when equation (2) is satisfied. In the case of the Tersoff model for Si, $\gamma_{sv} - \gamma_{lv}$ is about 50% larger than γ_{ls}, suggesting that the formation of a crystalline nucleus at the pressure minimum is hampered by the interfacial energy contribution to the free energy. To further confirm our analysis, we conducted more simulations for the liquid slab at 0.95 T_m. By restricting the sampling of nuclei only in the immediate vicinity of the surface (that is, by restricting nucleation to occur at the surface), we computed the growth probability of Si clusters with one facet exposed to the liquid–vacuum interface. The results (see Supplementary Information for details) show that the nucleus has a lower growth probability at the surface than in the subsurface region.

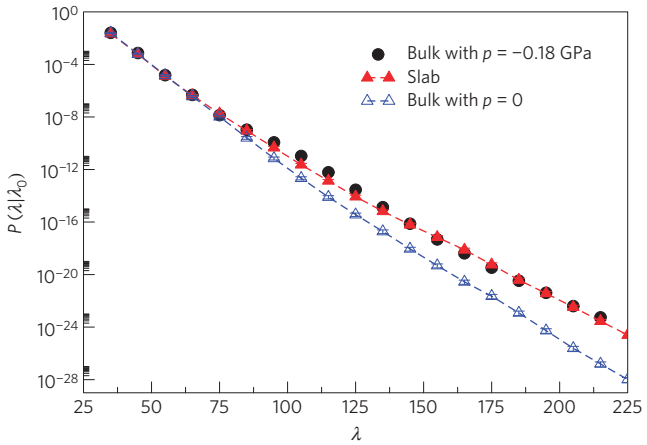

Figure 4 | Effect of *p* on the homogeneous nucleation rate in the bulk liquid at 0.95 T_m. A small negative *p*, with the same magnitude as that induced by surface tension in the liquid slab, is applied on the bulk liquid. The resulting growth probability (black filled circles) almost coincides with that obtained for the liquid slab (red filled triangle).

Our calculations demonstrate that free surfaces can be favourable sites for freezing in liquid Si and Ge. The surface-induced nucleation reported in our simulation is attributed to the lowering of the nucleation barrier when the sign of density change on freezing opposes the sign of surface tension. Our result is consistent with recent experiments and simulations[29,30] showing that liquid Ge can be vitrified by applying pressure, and recent simulations showing that nucleation occurs in the core of Lennard-Jones liquid droplets[31]. Experiments show that the density of crystalline Si is nearly constant[32] as a function of T near T_m (with only 0.5% increase from T_m to 0.79 T_m), whereas the density of the supercooled liquid monotonically increases and varies by about 2.5% from T_m to 0.79 T_m (ref. 33). In addition, the density difference between the solid and the liquid at T_m is as high as 11.5%, much larger than the one predicted by both Tersoff and Stillinger–Weber models. Therefore, the tendency of surface-induced nucleation in real Si should be enhanced with respect to the models considered here; that is, the ratio between the surface-induced and bulk crystallization probabilities should increase. Our results further suggest that surface-induced nucleation should also be observed in other tetrahedrally coordinated materials showing a density decrease on solidification. One interesting case is water, for which there is experimental evidence suggesting surface crystallization in water droplets suspended in clouds[8].

Methods

We carried out molecular dynamics simulations, within the isobaric–isothermal canonical ensembles (constant number, pressure and temperature) at zero pressure and the isothermal canonical ensembles (constant number, volume and temperature) for bulk and for slab configurations, respectively. A periodic boundary condition was used. In particular, the slab configuration was obtained by adding about 20 Å along z to the equilibrium configuration obtained from the constant number, pressure and temperature simulation. Most of our simulations were carried out with 5,832 atoms in a cubic cell, with the exception of our calculations of the distributions of solid Si clusters (Fig. 2), where we replicated the unit cell along the z direction and included 11,664 atoms. We use the local parameter q_3 (ref. 24), a quantity that is highly sensitive to crystalline order, to identify Si crystalline clusters in the liquid. To compute the flux rates $\dot{\Phi}_{\lambda_0}$, we conducted standard molecular dynamics simulations starting from a well-defined basin ($\lambda < \lambda_A$) in phase space. As occasional fluctuations lead to direct crossing of the first interface, λ_0, the atomic configuration is recorded. The simulation is then continued until a large number N_0 ($\sim$120) of configurations are collected and the average flux rate is given by $N_0/(t_0 V)$, where t_0 and V are the total simulation time and the system volume, respectively.

To compute the growth probability $P(\lambda|\lambda_0)$, we start from the configurations collected at the interface λ_0 and carry out a large number (M_1, typically around 1,000 $\sim$ 10,000) of trial molecular dynamics runs with different randomized initial momenta. A few (k_1) trial runs result in successful crossings to the next interface, whereas in the remaining cases small crystalline clusters dissolve. The individual crossing probability $P(\lambda|\lambda_0)$ is then given by k_1/M_1. The subsequent trial runs are fired at these crossing points on the next interface and so on, so that the total growth probability is given by: $P_{\lambda_n} = \prod_{i=1}^{n} P(\lambda_i|\lambda_{i-1})$. To evaluate the effect of sampling techniques on our results, we repeated our calculations of $P(\lambda|\lambda_0)$ at 0.95 T_m by using a Langevin thermostat[34] and by varying both the interface spacing and the cell size. The observed changes in nucleation rate are within the error bars given in Fig. 1a.

To estimate the critical size at 0.95 T_m, we assume the interface free energy remains a constant and the critical nucleus radius $r_c = \alpha/\Delta\mu$, where α is constant and $\Delta\mu = \mu_S - \mu_L$ is the difference in the chemical potential between the solid and the liquid. By expanding $\Delta\mu$ to the second order, that is, $\Delta\mu = ax + bx^2$, where $x = 1 - T/T_m$, and using the critical sizes at 0.79 T_m and 0.86 T_m (see Fig. 1a), one can estimate that the critical size λ^* at 0.95 T_m contains 5,900 $\sim$ 9,700 atoms, which yields $\delta G_v^*(p)$ to be around $-7\ k_B T \sim -11.5\ k_B T$, where k_B is the Boltzmann constant.

Received 6 April 2009; accepted 2 July 2009; published online 9 August 2009

References

1. van der Veen, J. Melting and freezing at surfaces. *Surf. Sci.* **433,** 1–11 (1999).
2. Lang, P. Surface induced ordering effects in soft condensed matter systems. *J. Phys. Condens. Matter* **16,** 699–720 (2004).
3. Regan, M. *et al.* Surface layering in liquid gallium: An X-ray reflectivity study. *Phys. Rev. Lett.* **75,** 2498–2501 (1995).
4. Shpyrko, O. *et al.* Surface crystallization in a liquid AuSi alloy. *Science* **313,** 77–80 (2006).
5. Sutter, P. & Sutter, E. Dispensing and surface-induced crystallization of zeptolitre liquid metal-alloy drops. *Nature Mater.* **6,** 363–366 (2007).
6. Zanotto, E. & Fokin, V. Recent studies of internal and surface nucleation in silicate glasses. *Phil. Trans. Math. Phys. Eng. Sci.* **361,** 591–613 (2003).
7. Schmelzer, J., Pascova, R., Moller, J. & Gutzow, I. Surface-induced devitrification of glasses: The influence of elastic strains. *J. Non-Cryst. Solids* **162,** 26–39 (1993).
8. Tabazadeh, A., Djikaev, Y. & Reiss, H. Surface crystallization of supercooled water in clouds. *Proc. Natl Acad. Sci. USA* **99,** 15873–15878 (2002).
9. Shaw, R., Durant, A. & Mi, Y. Heterogenous surface crystallization observed in undercooled water. *J. Phys. Chem. B* **109,** 9865–9868 (2005).
10. Sastry, S. Water: Ins and outs of ice nucleation. *Nature* **438,** 746–747 (2005).
11. Kim, B. *et al.* Kinetics of individual nucleation events observed in nanoscale vapour–liquid–solid growth. *Science* **322,** 1070–1073 (2008).
12. Moroni, D., ten Wolde, P. & Bolhuis, P. Interplay between structure and size in a critical crystal nucleus. *Phys. Rev. Lett.* **94,** 235703 (2005).
13. Auer, S. & Frenkel, D. Prediction of absolute crystal-nucleation rate in hard-sphere colloids. *Nature* **409,** 1020–1023 (2001).
14. Cacciuto, A., Auer, S. & Frenkel, D. Onset of heterogeneous crystal nucleation in colloidal suspensions. *Nature* **428,** 404–406 (2004).
15. Pluis, B., Frenkel, D. & van der Veen, J. Surface-induced melting and freezing II. A semiempirical Laudau-type model. *Surf. Sci.* **239,** 282–300 (1990).
16. Djikaev, Y., Tabazadeh, A., Hamill, P. & Reiss, H. Thermodynamic conditions for the surface-stimulated crystallization of atmospheric droplets. *J. Phys. Chem. A* **106,** 10247–10253 (2002).
17. Rice, S. Research overview: The liquid–vapour interface of a metal as a vehicle for studying the atomic, electronic, and optical properties of an inhomogeneous liquid. *Proc. Natl Acad. Sci. USA* **84,** 4709–4716 (1987).
18. Halka, V., Streitel, R. & Freyland, W. Is surface crystallization in liquid eutectic AuSi surface-induced? *J. Phys. Condens. Matter* **20,** 355007 (2008).
19. Allen, R., Frenkel, D. & ten Wolde, P. R. Simulating rare events in equilibrium or nonequilibrium stochastic systems. *J. Chem. Phys.* **124,** 024102 (2006).
20. Allen, R., Frenkel, D. & ten Wolde, P. R. Forward flux sampling-type schemes for simulating rare events: Efficiency analysis. *J. Chem. Phys.* **124,** 194111 (2006).
21. Voter, A. Parallel replica method for dynamics of infrequent events. *Phys. Rev. B* **57,** R13985 (1998).
22. Tersoff, J. Modeling solid-state chemistry: Interatomic potentials for multicomponent systems. *Phys. Rev. B* **39,** 5566–5568 (1989).
23. Stillinger, F. & Weber, T. Computer simulation of local order in condensed phases of silicon. *Phys. Rev. B* **31,** 5262–5271 (1985).
24. Ghiringhelli, L., Valeriani, C., Meijer, E. & Frenkel, D. Local structure of liquid carbon controls diamond nucleation. *Phys. Rev. Lett.* **99,** 055702 (2007).
25. Devaud, G. & Turnbull, D. Undercooling of molten silicon. *Appl. Phys. Lett.* **46,** 844–845 (1985).
26. Lee, B., Kuranaga, T., Munetoh, S. & Motooka, T. Surface nucleation of the (111) plane of excimer laser annealed Si on SiO_2 substrates: A molecular dynamics study. *J. Appl. Phys.* **101,** 054316 (2007).
27. Tang, Y., Wang, J. & Zeng, X. Molecular simulations of solid–liquid interfacial tension of silicon. *J. Chem. Phys.* **124,** 236103 (2006).

28. Kelton, K. in *Solid State Physics-Advances in Research and Applications* Vol. 45 (eds Ehrenreich, H. & Turnbull, D.) 75–178 (Academic, 1991).
29. Bhat, M. *et al*. Vitrification of a monotomic metallic liquid. *Nature* **448,** 787–790 (2007).
30. Molinero, V., Sastry, S. & Angell, C. Tuning of tetrahedrality in a silicon potential yields a series of monatomic (metal-like) glass formers of very high fragility. *Phys. Rev. Lett.* **97,** 075701 (2006).
31. van Meel, J., Page, A., Sear, R. & Frenkel, D. Two-step vapour-crystal nucleation close below triple point. *J. Chem. Phys.* **129,** 204505 (2008).
32. Stankus, S., Khairulin, R. & Tyagelskii, P. The thermal properties of germanium and silicon in condensed state. *High Temp.* **37,** 529–534 (1999).
33. Morishita, T. How does tetrahedral structure grow in liquid silicon upon supercooling? *Phys. Rev. Lett.* **97,** 165502 (2006).
34. Chandrasekhar, S. Stochastic problems in physics and astronomy. *Rev. Mod. Phys.* **15,** 1–89 (1943).

Acknowledgements

We gratefully thank D. C. Chrzan, A. F. Voter and M. Parrinello for fruitful discussions. This work was supported by DOE/BES (contract number DE-FG02-06ER46262).

Author contributions

T.L., D.D. and G.G. designed the research, interpreted results and wrote the paper; T.L. and D.D. designed and implemented the method and analysed results; T.L. carried out calculations; L.M.G. discussed initial design and implementation of the research.

Additional information

Supplementary information accompanies this paper on www.nature.com/naturematerials. Reprints and permissions information is available online at http://npg.nature.com/reprintsandpermissions. Correspondence and requests for materials should be addressed to T.L.